

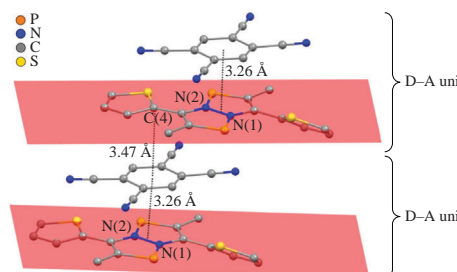
2-Thienyl-substituted 3a,6a-diaza-1,4-diphosphapentalene: synthesis and complexation with 1,2,4,5-tetracyanobenzene

Matvey D. Grishin, Natalia V. Zolotareva, Yuliya S. Panova, Vyacheslav V. Sushev,
Roman V. Rumyantcev, Georgy K. Fukin and Alexander N. Kornev*

*G. A. Razuvayev Institute of Organometallic Chemistry, Russian Academy of Sciences,
603137 Nizhny Novgorod, Russian Federation. E-mail: akornev@iomc.ras.ru*

DOI: 10.1016/j.mencom.2023.09.013

Synthesis of 2,5-dimethyl-3,6-di(2-thienyl)-3a,6a-diaza-1,4-diphosphapentalene was accomplished. Interaction of this compound with 1,2,4,5-tetracyanobenzene afforded black crystals of the 1:1 adduct containing π -stacks of D–A units with short interplanar spacing of 3.26 Å inside the unit and 3.47 Å between the D–A units, where tetracyanobenzene is an acceptor of 0.2 e. Estimation of the HOMO–LUMO gap from the onset of optical absorption gave value of 1.28 eV.



Keywords: diazadiphosphapentalenes, charge-transfer complexes, phosphinidenes, 1,2,4,5-tetracyanobenzene, X-ray diffraction, electronic spectroscopy, cyclic voltammetry.

Charge-transfer complexes occupy an important place among organic conducting materials. The degree of charge transfer, the electronic and optical properties of the complexes are determined by the specifics of the donor and acceptor.^{1–3} Polycyano compounds are used as traditional π -acceptors of electron density.^{4–8} As for π -donors, the leading positions today are steadily held by tetrathiafulvalene derivatives.^{9–12} The introduction of easily polarizable atoms (S, Se, Te) into the donor molecule significantly increases the mobility of charge carriers. However, the problem of mobility remains, and the search for new effective donors for the creation of materials for electronics is still promising. We have recently found that compounds belonging to a new class of phosphorus–nitrogen heterocycles, 3a,6a-diaza-1,4-diphosphapentalenes (DDPs), have powerful π -donor properties. They easily form complexes with a typical π -acceptor such as 1,2,4,5-tetracyanobenzene (TCNB).^{13,14} The donor properties of DDPs are especially pronounced in comparison with their closest relatives, (di)azaphospholes,¹⁵ which are not active even towards such strong electrophiles as boron halides. The reason for the high donor activity of DDPs is that they are masked singlet phosphinidenes with a high energy of the highest occupied molecular orbital localized on the π -system.¹⁶ The equilibrium in Figure 1 reflects

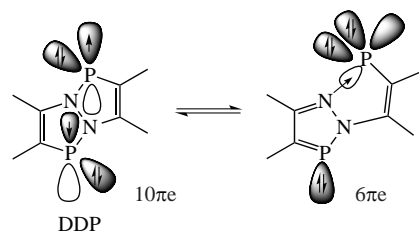


Figure 1 Electron shell transformation in the DDP system caused by an external polarizing impact (weak Lewis acid, polar solvent, or a second DDP molecule).

the dual nature of DDPs which can exhibit the properties of both heterocycles (complexation with π -acceptors,^{13,14} cycloaddition,¹⁷ rearrangements¹⁸) and stabilized singlet phosphinidenes (oligomerization,¹⁶ complexation with Lewis acids,¹⁹ oxidative addition²⁰).

To date, we have identified two types of DDP complexes with TCNB, which differ in stoichiometry and molecular packing in the crystal. The first type includes TCNB complexes with diazadiphosphapentalenes **1** and **2**, in which the donor and acceptor form infinite stacks of 1:1 composition (Figure 2).

Diazadiphosphapentalenes **3** and **4** form 2:1 complexes with TCNB. In crystals of such complexes, infinite chains with short P···P contacts are observed. In this communication, we present information about the synthesis of diazadiphosphapentalene with 2-thienyl peripheral substituents and its complexation with

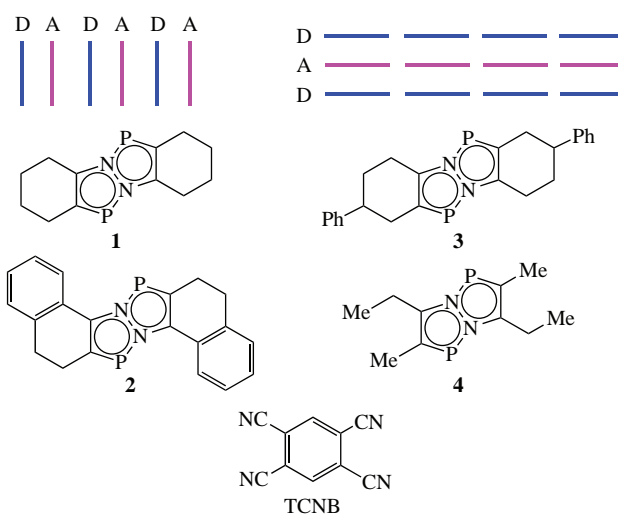
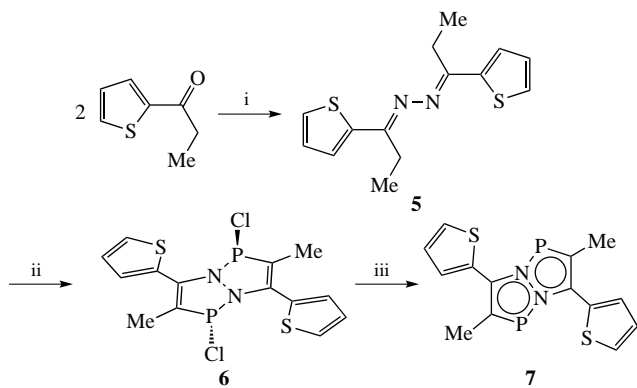


Figure 2 Schematic representations of DA complexes with different structural modes. D = **1–4**, A = TCNB.



Scheme 1 Reagents and conditions: i, $\text{N}_2\text{H}_4\cdot\text{H}_2\text{O}$ (1.0 equiv.); ii, PCl_3 , 80 °C, 3–4 h; iii, Mg, THF, room temperature, 8 h.

TCNB, namely, discussing the crystal packing of the complexes, the degree of charge transfer, and spectral characteristics. The synthetic route to thiophenyl-substituted DDP is shown in Scheme 1.

1-(2-Thienyl)propan-1-one azine **5** was prepared in 75% yield by the action of hydrazine hydrate on the corresponding ketone. Subsequent heating of azine **5** with phosphorus trichloride at 80 °C is accompanied by the evolution of gaseous HCl and the formation of diazadiphosphapentalene dichloride **6**. Free diazadiphosphapentalene **7** was obtained by reduction of dichloride **6** with magnesium powder in THF in 83% yield. This is burgundy crystalline powder insensitive in solid state to oxygen and atmospheric moisture.

For compounds **5–7**, X-ray diffraction analysis was performed.[†] Azine **5** crystallizes exclusively as an *E,E*-isomer containing a flat azine skeleton, in which the thiophenyl substituents have a slight slope (13.24°) to this plane, and the ethyl groups are located on opposite sides, respectively (see Online Supplementary Materials, Figure S1). Dichloride **6** was isolated as yellow moisture-sensitive crystals. Compound **6** crystallizes as the *trans* isomer like the vast majority of DDP-dichlorides (Figure S2), its heteropentalene framework has a nonplanar geometry with the deviation of atoms from the averaged plane up to 0.191 Å (mean deviation 0.063 Å). Thiophenyl-substituted diazadiphosphapentalene **7** has a heteropentalene framework geometry close to planar (Figure 3) with an average deviation of

[†] Crystal data for **5**. $\text{C}_{14}\text{H}_{16}\text{N}_2\text{S}_2$, orthorhombic, space group $\text{P}b\text{ca}$, 150(2) K, $a = 9.3123(3)$, $b = 8.7875(3)$ and $c = 16.9206(5)$ Å, $V = 1384.63(8)$ Å³, $Z = 4$, $d_{\text{calc}} = 1.326$ g cm⁻³, $\mu = 0.368$ mm⁻¹, $R_1 = 0.0333$ [from 1683 unique reflections with $I > 2\sigma(I)$] and $wR_2 = 0.0933$ (from all 2014 unique reflections).

Crystal data for **6**. $\text{C}_{14}\text{H}_{12}\text{Cl}_2\text{N}_2\text{P}_2\text{S}_2$, triclinic, space group $\bar{\text{P}1}$, 298(2) K, $a = 9.8471(5)$, $b = 9.9315(4)$ and $c = 10.0018(6)$ Å, $\alpha = 90.203(4)$, $\beta = 106.333(5)$ and $\gamma = 115.800(5)$ °, $V = 836.07(8)$ Å³, $Z = 2$, $d_{\text{calc}} = 1.610$ g cm⁻³, $\mu = 0.825$ mm⁻¹, $R_1 = 0.0441$ [from 3264 unique reflections with $I > 2\sigma(I)$] and $wR_2 = 0.1194$ (from all 4858 unique reflections).

Crystal data for **7**. $\text{C}_{14}\text{H}_{12}\text{N}_2\text{P}_2\text{S}_2$, triclinic, space group $\bar{\text{P}1}$, 298(2) K, $a = 7.43678(16)$, $b = 8.0174(2)$ and $c = 12.3653(3)$ Å, $\alpha = 81.729(2)$, $\beta = 81.0510(18)$ and $\gamma = 89.261(2)$ °, $V = 720.68(3)$ Å³, $Z = 2$, $d_{\text{calc}} = 1.541$ g cm⁻³, $\mu = 0.580$ mm⁻¹, $R_1 = 0.0416$ [from 3130 unique reflections with $I > 2\sigma(I)$] and $wR_2 = 0.1210$ (from all 3709 unique reflections).

Crystal data for **8**. $\text{C}_{24}\text{H}_{14}\text{N}_6\text{P}_2\text{S}_2$, monoclinic, space group $\text{P}2_1/c$, 150(2) K, $a = 8.1729(2)$, $b = 7.3202(2)$ and $c = 37.6319(11)$ Å, $\beta = 94.500(3)$ °, $V = 2244.48(11)$ Å³, $Z = 4$, $d_{\text{calc}} = 1.517$ g cm⁻³, $\mu = 0.407$ mm⁻¹, $R_1 = 0.0484$ [from 7069 unique reflections with $I > 2\sigma(I)$] and $wR_2 = 0.1181$ (from all 10368 unique reflections).

CCDC 2255159 (**5**), 2255160 (**6**), 2255161 (**7**) and 2255162 (**8**) contain the supplementary crystallographic data for this paper. These data can be obtained free of charge from The Cambridge Crystallographic Data Centre via <http://www.ccdc.cam.ac.uk>.

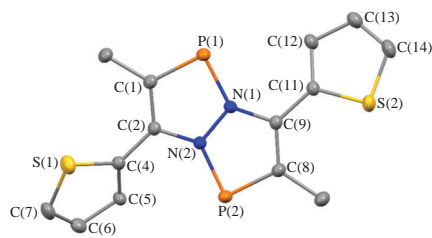


Figure 3 Molecular structure of compound **7**. Thermal ellipsoids drawn at the 30% probability level. Hydrogen atoms are omitted for clarity. Selected bond lengths (Å) and angles (°): P(1)–N(1) 1.7346(15), P(1)–C(1) 1.7350(19), N(1)–N(2) 1.377(2), N(2)–C(2) 1.385(2), C(1)–C(2) 1.385(2), C(8)–C(9) 1.387(2), S(1)–C(7) 1.697(3), S(1)–C(4) 1.7165(19); N(1)–P(1)–C(1) 89.13(8), N(1)–N(2)–C(2) 112.06(14), N(2)–N(1)–P(1) 113.42(12), N(1)–N(2)–P(2) 114.69(12).

atoms from the averaged plane of 0.046 Å and a maximum deviation of 0.070 Å at the N(2) atom. The tilt angles between the thiophenyl and DDP planes are 41.9 and 24.2° for substituents containing S(1) and S(2), respectively. The carbon–carbon bonds of the heteropentalene fragment [C(1)–C(2) 1.385(2) Å, C(8)–C(9) 1.387(2) Å] are elongated in comparison with similar bonds in dichloride **6**, which corresponds to aromatization of this system. Molecules of **7** in the crystal are arranged in pairs with short contacts P–P 3.468 Å inside the pair (Figure S3).

The NMR spectra confirm the structure of the obtained compounds, but make some adjustments to their state in solution. The $^{31}\text{P}\{^1\text{H}\}$ NMR spectrum of dichloride **6** in THF shows two singlets (114.6, 118.7) corresponding to the presence in the solution of *cis*- and *trans*-isomers that differ in the position of chlorine atoms relative to the plane of the heteropentalene framework. The methyl groups in compound **6** instead of the expected doublet ($^3J_{\text{H},\text{P}}$) in the ^1H NMR spectrum resonate as multiplet which in the $^1\text{H}\{^{31}\text{P}\}$ NMR spectrum turns into a singlet at 2.19 ppm. Diazadiphosphapentalene **7** has a singlet in the $^{31}\text{P}\{^1\text{H}\}$ NMR spectrum in the predicted downfield region at 192.1 ppm, while the ^{31}P NMR spectrum shows a quartet with $^3J_{\text{H},\text{P}} = 13.6$ Hz. Accordingly, the methyl group appears in the ^1H NMR spectrum as a doublet at 2.5 ppm with $^3J_{\text{H},\text{P}} = 13.9$ Hz.

Electrochemical behavior of compounds **6** and **7** were investigated by cyclic voltammetry. On the cathode branch of cyclic voltammogram of **6**, the first broadened wave at -1.64 V is irreversible, obviously, is the result of reduction of two

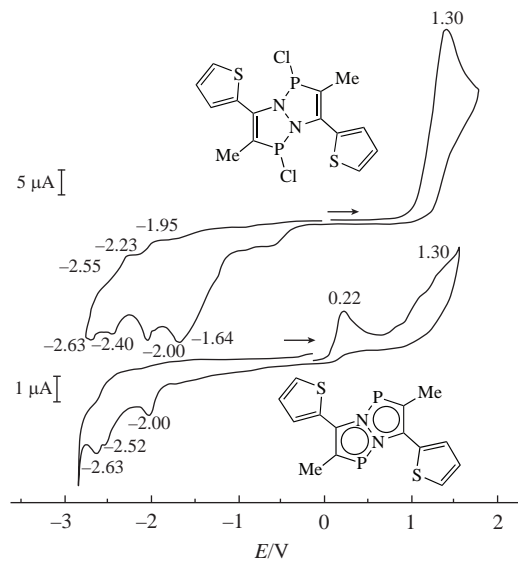


Figure 4 Cyclic voltammetry of **6** (top) and **7** (bottom) in DMF, 0.1 M Bu_4NPF_6 , $v = 100$ mV s⁻¹, glassy carbon 1 mm, potentials vs. Ag/AgCl.

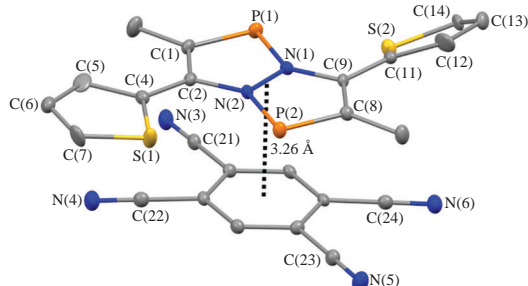


Figure 5 Molecular structure of D–A unit in **8**. Thermal ellipsoids drawn at the 30% probability level. Hydrogen atoms are omitted for clarity. Selected bond lengths (Å) and angles (°): P(1)–N(1) 1.721(2), P(1)–C(1) 1.726(3), N(1)–N(2) 1.393(3), N(2)–C(2) 1.394(3), C(1)–C(2) 1.385(3), N(3)–C(21) 1.144(3), N(4)–C(22) 1.138(3), N(5)–C(23) 1.139(3), N(6)–C(24) 1.145(3); N(1)–P(1)–C(1) 88.84(11), N(2)–N(1)–P(1) 114.27(15), N(1)–N(2)–C(2) 111.01(19), N(3)–C(21)–C(15) 179.2(3).

P–Cl bonds (Figure 4). The second and subsequent reduction waves (−2.00, −2.40, −2.63 V) correspond to the processes of quasi-reversible or irreversible addition of electrons to the DDP fragment, which is consistent with the data for the corresponding DDP **7**. In the anodic sweep, DDP **7** has oxidation peak potential at 0.22 V. Such a low value of the potential indicates a high donor ability of the resulting diazadiphosphapentalene, which manifests itself in its complexation with 1,2,4,5-tetracyanobenzene.

Diazadiphosphapentalene **7** in THF solution reacts with TCNB at room temperature to form an oxygen-resistant black crystalline product **8**. It was found that carrying out the reactions in an equimolar ratio or with an excess of TCNB leads to the complex having a composition DDP/TCNB = 1 : 1. Crystals of **8** suitable for X-ray diffraction analysis were grown from a slowly cooling THF solution. The molecular structure of the donor-acceptor (D–A) unit of **8** is shown in Figure 5.

In the crystal, the donor (DDP) and acceptor (TCNB) molecules are combined in D–A units which form infinite stacks (Figure 6).

The donor and acceptor molecules of neighboring stacks AA or BB lie in the same plane and have short contacts C_{SP2}–H···N≡C (Figure S4). At the same time, the layers of molecules in neighboring stacks AB are located at an angle of 51.2° (Figure S5), and also interact through short contacts C_{SP2}–H···N≡C. The distance between the midplane of the DDP and the centre of the TCNB molecule in the D–A units is 3.262 Å. In turn, the distance between D–A units is 3.469 Å. These geometrical parameters are suitable for the realization of intermolecular π···π-interactions.²¹

To estimate the charge transfer from DDP molecules to TCNB, we have carried out a theoretical study of the electron density topology in **8** within the framework of Bader theory²² (see Online Supplementary Materials for the methodology).

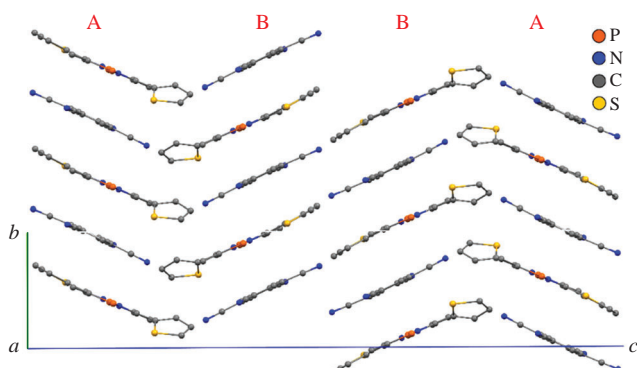


Figure 6 Location of stacks (–DDP–TCNB–) in complex **8** along the crystallographic axis *b*.

According to the calculations, each TCNB molecule is an acceptor of 0.2 e in crystal. Note that the analogous value for complex **4** with TCNB (2 : 1) was 0.3 e.¹⁴ The lower value for **8** correlates with longer distances between donor and acceptor molecules (3.26 and 3.47 Å) compared to (4)₂(TCNB) (both 3.25 Å).

Analysis of the theoretical molecular graph has revealed the presence of intermolecular interactions between DDP and TCNB molecules (Figure S6). Within the D–A unit, the energy of intermolecular interactions is 6.3 kcal mol^{−1}, whereas between D–A units it is 3.5 kcal mol^{−1}.²³ This phenomenon agrees with the difference in the distances between the donor and acceptor molecules in the stacks. It should be noted that there are intramolecular interactions in DDP between phosphorus and sulfur atoms whose energies are 2.5 kcal mol^{−1} [for P(1)···S(2) interaction] and 3.1 kcal mol^{−1} [for P(2)···S(1) interaction]. The main topological characteristics of the electron density in the complex **8** are shown in Table S1.

All cyano groups in the acceptor molecule differ in the length of C–N bonds, which are in the range of 1.138(3)–1.145(3) Å. Meanwhile, the frequency of C≡N stretching vibrations can be used to estimate the degree of charge transfer (DCT) between the donor and acceptor. The equation for DCT calculation by IR spectrum is: DCT = $2\Delta\nu/\nu_0(1 - \nu_1^2/\nu_0^2)^{-1}$.^{24,25} The ν_0 , ν_{CT} and ν_1 represent C≡N stretching modes frequency of the pure TCNB, charge transfer compound and the TCNB anion, respectively. For TCNB, $\nu_0 = 2245$ cm^{−1}, $\nu_1 = 2198$ cm^{−1}, while for complex **8**, two frequencies were observed, 2240 and 2225 cm^{−1}, with red shift of 5 and 20 cm^{−1}, respectively (Figure S7). The frequency shift of 20 cm^{−1} is the largest value found to date for DDP complexes with TCNB. Calculations for these frequencies thus give values 0.1 and 0.4 e. The occurrence of two CN vibration bands in the spectrum of complex **8** correlates with the presence of two π-donor blocks (DDP, C₄H₃S), which differ in π-donor activity. The absorption bands $\nu_{(CH)}$ 3028 and 3105 cm^{−1} found for **8** shifted to lower values from those for free TCNB (3048 and 3113 cm^{−1}) and are indicative of charge transfer also.

The electronic absorption spectrum of complex **8** shows a long-wavelength band at 780 nm (Figure S10) vs. $\lambda_{\text{max}} = 457$ nm for the original DDP (Figure S11). The HOMO–LUMO gap found from the onset of optical absorption is 1.28 eV. The UV–Vis spectrum of **8** measured in thin film (Nujol) contains a new, longer wavelength absorption band at 913 nm (Figure S12). It is clear that not the entire 3D coordination polymer (complex **8**) passes into the CD₂Cl₂ solution, but only its fragment. Therefore, the HOMO–LUMO gap for solid **8** can be estimated to be less than 1.0 eV.

In summary, a 1 : 1 charge-transfer complex of thiényl-substituted 3a,6a-diaza-1,4-diphosphapentalene with 1,2,4,5-tetracyanobenzene was synthesized. The donor and acceptor molecules form tilted stacks of D–A units with intermolecular distances of 3.262 Å inside the unit and 3.469 Å between the units. The study of the electron density topology showed that each TCNB molecule is an acceptor of 0.2 e in the crystal. An estimate of the HOMO–LUMO energy gap by electron absorption spectroscopy gave a value of 1.28 eV in solution and ~1.0–0.9 eV when measured in a film.

This work was supported by the Russian Science Foundation (grant no. 19-13-00400-P) and performed using the equipment of the center for collective use ‘Analytical Center of the IOMC RAS’ with the financial support of the grant ‘Ensuring the development of the material and technical infrastructure of the centers for collective use of scientific equipment’ (Unique identifier RF-2296.61321X0017, Agreement no. 075-15-2021-670). Theoretical electron density research was

supported by the Russian Science Foundation (grant no. 21-13-00336).

Online Supplementary Materials

Supplementary data associated with this article can be found in the online version at doi: 10.1016/j.mencom.2023.09.013.

References

- 1 E. A. Chulanova, N. A. Semenov, N. A. Pushkarevsky, N. P. Gritsan and A. V. Zibarev, *Mendeleev Commun.*, 2018, **28**, 453.
- 2 D. V. Konarev, *Mendeleev Commun.*, 2020, **30**, 249.
- 3 A. V. Maleeva, I. V. Ershova, O. Yu. Trofimova, K. V. Arsenyeva, I. A. Yakushev and A. V. Piskunov, *Mendeleev Commun.*, 2022, **32**, 83.
- 4 V. A. Starodub and T. N. Starodub, *Russ. Chem. Rev.*, 2014, **83**, 391.
- 5 J. Zhang, W. Xu, P. Sheng, G. Zhao and D. Zhu, *Acc. Chem. Res.*, 2017, **50**, 1654.
- 6 E. W. Reinheimer, M. Fernandez, B. Rivas, H. Zhao and K. R. Dunbar, *J. Chem. Crystallogr.*, 2011, **41**, 936.
- 7 S. P. Fisher and E. W. Reinheimer, *J. Chem. Crystallogr.*, 2014, **44**, 161.
- 8 J. D. Bagnato, W. W. Shum, M. Strohmeier, D. M. Grant, A. M. Arif and J. S. Miller, *Angew. Chem., Int. Ed.*, 2006, **45**, 5322.
- 9 D. Jérôme, *Chem. Rev.*, 2004, **104**, 5565.
- 10 S. Goeb and M. Sallé, *Acc. Chem. Res.*, 2021, **54**, 1043.
- 11 M. Mas-Torrent and C. Rovira, *J. Mater. Chem.*, 2006, **16**, 433.
- 12 K. P. Goetz, D. Verneulen, M. E. Payne, C. Kloc, L. E. McNeil and O. D. Jurchescu, *J. Mater. Chem. C*, 2014, **2**, 3065.
- 13 Y. S. Panova, V. V. Sushev, D. F. Dorado Daza, N. V. Zolotareva, R. V. Rumyantcev, G. K. Fukin and A. N. Kornev, *Inorg. Chem.*, 2020, **59**, 11337.
- 14 N. Zolotareva V. Sushev, Y. Panova, A. Khristolyubova, M. Grishin, R. Rumyantcev, G. Fukin and A. Kornev, *ChemPlusChem*, 2023, **88**, e202200438.
- 15 R. K. Bansal, N. Gupta and S. K. Kumawat, *Curr. Org. Chem.*, 2007, **11**, 33.
- 16 A. N. Kornev, Y. S. Panova, V. V. Sushev, D. F. Dorado Daza, A. S. Novikov, A. V. Cherkasov, G. K. Fukin and G. A. Abakumov, *Inorg. Chem.*, 2019, **58**, 16144.
- 17 A. N. Kornev, V. E. Galperin, Yu. S. Panova, V. V. Sushev, A. V. Cherkasov, A. V. Arapova and G. A. Abakumov, *Russ. Chem. Bull.*, 2018, **67**, 2073.
- 18 Y. S. Panova, A. V. Khristolyubova, V. V. Sushev, N. V. Zolotareva, E. V. Baranov, G. K. Fukin and A. N. Kornev, *New J. Chem.*, 2021, **45**, 18491.
- 19 Y. Panova, A. Khristolyubova, N. Zolotareva, V. Sushev, V. Galperin, R. Rumyantcev, G. Fukin and A. Kornev, *Dalton Trans.*, 2021, **50**, 5890.
- 20 A. N. Kornev, V. E. Galperin, V. V. Sushev, N. V. Zolotareva, E. V. Baranov, G. K. Fukin and G. A. Abakumov, *Eur. J. Inorg. Chem.*, 2016, **22**, 3629.
- 21 C. Janiak, *J. Chem. Soc., Dalton Trans.*, 2000, **21**, 3885.
- 22 R. F. W. Bader, *Atoms in Molecules: A Quantum Theory*, Clarendon Press, Oxford, 1990.
- 23 E. Espinosa, E. Molins and C. Lecomte, *Chem. Phys. Lett.*, 1998, **285**, 170.
- 24 B. Mahns, O. Kataeva, D. Islamov, S. Hampel, F. Steckel, C. Hess, M. Knupfer, B. Büchner, C. Himeinschi, T. Hahn, R. Renger and J. Kortus, *Cryst. Growth Des.*, 2014, **14**, 1338.
- 25 P. Hu, K. Du, F. Wei, H. Jiang and C. Kloc, *Cryst. Growth Des.*, 2016, **16**, 3019.

Received: 22nd May 2023; Com. 23/7176